

Errata for “Analytical Model for the Impulse of Single-Cycle Pulse Detonation Tube” (Wintenberger et al., *Journal of Propulsion and Power*, Vol. 19, No. 1, pp. 22–38, 2003).

E. Wintenberger*, J. M. Austin†, M. Cooper‡, S. Jackson§, J. E. Shepherd¶
California Institute of Technology, Pasadena, California 91125

Errata

In the original evaluation of our analytical model for the single-cycle impulse of a pulse detonation tube,¹ we approximated the detonation product isentrope as having a frozen composition with a corresponding polytropic exponent γ_f . As discussed in the accompanying comment by Radulescu and Hanson and our response, for many situations, it is more appropriate to use an equilibrium approximation to the isentrope. This implies a different value of the polytropic exponent $\gamma = \gamma_e$, a new computational procedure for computing the plateau pressure P_3 , and results in revised values for the predicted impulse.

Although the general equations and the qualitative conclusions drawn in our paper are unchanged, the revised numerical values of the predicted impulse differ up to 9.5% for stoichiometric fuel-oxygen mixtures and less than 1.3% for fuel-air mixtures at standard conditions. In this errata, we present a revised set of selected tables and figures along with a short description of the calculations. The choice of the isentropic exponent, issues associated with chemical equilibrium, and the relevance to impulse calculations are discussed in the associated comment by Radulescu and Hanson and in our response to them.

The input parameters of our impulse model consist of the external pressure P_0 , the detonation velocity U_{CJ} , the equilibrium speed of sound behind the detonation front c_2 , the CJ pressure P_2 , and an approximation to the equilibrium polytropic exponent γ_e for the adiabatic expansion of the detonation products. All parameters were computed using numerical equilibrium calculations² performed with a realistic set of combustion products. Instead of the analytic computation used in our original paper, our revised properties at state 3 (behind the Taylor wave) are now calculated by numerically integrating the Riemann invariant along the equilibrium isentrope until the plateau region of no flow is reached.

$$\int_{P_3}^{P_2} \frac{dP}{\rho c} = u_2 . \quad (1)$$

*Post-doctoral Scholar, Aeronautics, Caltech MC 205-45, Pasadena, CA 91125, Member AIAA

†Assistant Professor, Aerospace Engineering, University of Illinois, Urbana, IL 61801, Member AIAA

‡Graduate Student, Mechanical Engineering, Caltech MC 205-45, Pasadena, CA 91125, Member AIAA

§Graduate Student, Aeronautics, Caltech MC 205-45, Pasadena, CA 91125, Member AIAA

¶Professor, Aeronautics, Caltech MC 105-50, Pasadena, CA 91125, Member AIAA

F. Pintgen developed the technique and automation which enabled us to compute the equilibrium isentropes and carry out the integration with the trapezoidal rule for the hundreds of cases considered in our study. A minimum of 200 increments was used in the evaluation of the plateau pressure. These parameters, along with γ_e evaluated at the CJ point, were then used in Eq. 19 of our paper¹ to calculate the parameter α , and the value of P_3 obtained from the numerical integration is used in Eq. 8 of our paper¹ to obtain the impulse. We have found that this procedure is superior to using a constant value of $\gamma = \gamma_e$ with the original analytic formulas, Eqs. 12 and 13, to obtain P_3 .

Figure 1 compares our impulse predictions with direct experimental impulse measurements of Cooper et al.,³ and is the revised version of Fig. 12 in our paper.¹ Using the revised values improves the agreement of the model predictions with the experimental data for cases with no obstacles.

Table 1 compares the revised values of our impulse predictions with those of the model of Zitoun and Desbordes⁴ for selected mixtures. Our revised impulse values are higher than the original values by less than 10% for fuel-oxygen mixtures but are virtually unchanged for fuel-air mixtures. Zitoun and Desbordes's predictions are still about 20% higher due to the difference in time of integration.¹

Values of the CJ parameters, γ_e , and revised model impulses for several stoichiometric fuel-oxygen-nitrogen mixtures are given in Table 2. The parameter q_c is the heat of combustion of the mixture per unit mass, whereas the parameter q is an effective energy release calculated using Eq. 45 in our paper.¹ Values of q given in Table 2 were computed using the one- γ detonation model⁵ with a gas constant based on the reactant molar mass. Note that the values of q computed in this fashion are significantly less than the heat of combustion q_c when the CJ temperature is above 3500 K due to dissociation of the major products. The values of q in Table 2 calculated for highly diluted mixtures can be higher than q_c because of the approximations made in using the one- γ model to calculate q . In general, the ratio of the effective energy release to the heat of combustion q/q_c decreases with increasing CJ temperature due to the higher degree of dissociation.

Using the revised values of $\gamma = \gamma_e$ also affected the value of the scaling parameter used to correlate the mixture-based specific impulse to the square root of the effective energy release (Eq. 44 in our paper¹). The range of γ_e for the mixtures considered (Table 2) was $1.133 < \gamma_e < 1.166$. The resulting coefficient of proportionality in Eq. 44 of our paper¹ is between 0.054 and 0.061 with an average value of 0.058 when q is expressed in J/kg, so that $I_{sp} \approx 0.058\sqrt{q}$. This relationship is tested in Fig. 2, which is the revised version of Fig. 16 in our paper.¹ The agreement between the model specific impulse and the approximate square root scaling relationship is improved compared to the original case.¹

The revised values of the mixture-based specific impulse are given for a wide range of fuels as a function of initial pressure (Fig. 3, revised version of Fig. 20 in our paper¹), equivalence ratio (Fig. 4, revised version of Fig. 21 in our paper¹), and nitrogen dilution (Fig. 5, revised version of Fig. 22 in our paper¹). The fuel-based specific impulse and the impulse per unit volume can easily be deduced from the mixture-based specific impulse. The revised numerical values for all these parameters are available in Wintenberger.⁶ The predicted values of the mixture-based specific impulse are on the order of 155 to 165 s for stoichiometric hydrocarbon-oxygen mixtures, 190 s for hydrogen-oxygen, and on the order of 115–125 s for fuel-air mixtures at initial conditions of 1 bar and 300 K.

References

¹Wintenberger, E., Austin, J., Cooper, M., Jackson, S., and Shepherd, J. E., “Analytical Model for the Impulse of Single-Cycle Pulse Detonation Tube,” *Journal of Propulsion and Power*, Vol. 19, No. 1, 2003, pp. 22–38.

²Reynolds, W., “The Element Potential Method for Chemical Equilibrium Analysis: Implementation in the Interactive Program STANJAN,” Tech. rep., Mechanical Engineering Department, Stanford University, 1986.

³Cooper, M., Jackson, S., Austin, J., Wintenberger, E., and Shepherd, J. E., “Direct Experimental Impulse Measurements for Deflagrations and Detonations,” *Journal of Propulsion and Power*, Vol. 18, No. 5, 2002, pp. 1033–1041.

⁴Zitoun, R. and Desbordes, D., “Propulsive Performances of Pulsed Detonations,” *Comb. Sci. Tech.*, Vol. 144, 1999, pp. 93–114.

⁵Thompson, P. A., *Compressible Fluid Dynamics*, Advanced Engineering Series, Rensselaer Polytechnic Institute, pp. 347–359, 1988.

⁶Wintenberger, E., *Application of Steady and Unsteady Detonation Waves to Propulsion*, Ph.D. thesis, California Institute of Technology, Pasadena, California, 2004.

List of Tables

1	Comparison of the model predictions for the mixture-based specific impulse.	5
2	Detonation CJ parameters and computed impulse for selected stoichiometric mixtures at 1 bar initial pressure and 300 K initial temperature.	6

Mixture	Model I_{sp} (s)	Zitoun and Desbordes ⁴ (s)
$C_2H_4+3O_2$	164	200
$C_2H_4+3(O_2+3.76N_2)$	118	142
$C_2H_2+2.5O_2$	167	203
$C_2H_2+2.5(O_2+3.76N_2)$	122	147
$H_2+0.5O_2$	189	226
$H_2+0.5(O_2+3.76N_2)$	124	149

Table 1: Comparison of the model predictions for the mixture-based specific impulse.

Mixture	q_c (MJ/kg)	γ_e	P_2 (bar)	T_2 (K)	U_{CJ} (m/s)	M_{CJ}	I_{sp} (s)	q (MJ/kg)
H ₂ -O ₂	13.3	1.129	18.7	3679	2840	5.26	189	11.0
H ₂ -O ₂ -20% N ₂	8.39	1.131	18.0	3501	2474	5.16	164	8.16
H ₂ -O ₂ -40% N ₂	5.20	1.141	16.9	3256	2187	5.01	142	5.93
H ₂ -air	3.39	1.163	15.5	2948	1971	4.81	124	4.17
C ₂ H ₂ -O ₂	11.8	1.153	33.6	4209	2424	7.32	167	7.45
C ₂ H ₂ -O ₂ -20% N ₂	9.60	1.150	30.2	4051	2311	6.89	157	6.69
C ₂ H ₂ -O ₂ -40% N ₂	7.31	1.150	26.5	3836	2181	6.42	148	5.95
C ₂ H ₂ -O ₂ -60% N ₂	4.95	1.152	22.5	3505	2021	5.87	134	4.93
C ₂ H ₂ -air	3.39	1.163	19.2	3147	1879	5.42	122	3.93
C ₂ H ₄ -O ₂	10.7	1.140	33.3	3935	2376	7.24	164	7.74
C ₂ H ₄ -O ₂ -20% N ₂	8.70	1.137	29.6	3783	2258	6.79	156	7.05
C ₂ H ₄ -O ₂ -40% N ₂	6.66	1.137	25.9	3589	2132	6.32	146	6.16
C ₂ H ₄ -O ₂ -60% N ₂	4.53	1.143	21.8	3291	1977	5.77	131	4.99
C ₂ H ₄ -air	3.01	1.161	18.2	2926	1825	5.27	118	3.73
C ₃ H ₈ -O ₂	10.0	1.134	36.0	3826	2360	7.67	165	8.24
C ₃ H ₈ -O ₂ -20% N ₂	8.33	1.133	31.7	3688	2251	7.14	155	7.44
C ₃ H ₈ -O ₂ -40% N ₂	6.48	1.134	27.4	3513	2131	6.58	146	6.47
C ₃ H ₈ -O ₂ -60% N ₂	4.49	1.141	22.8	3239	1980	5.95	133	5.18
C ₃ H ₈ -air	2.80	1.166	18.2	2823	1801	5.29	116	3.57
JP10-O ₂	9.83	1.138	38.9	3899	2294	7.99	161	7.67
JP10-O ₂ -20% N ₂	8.34	1.135	34.0	3759	2204	7.41	153	7.08
JP10-O ₂ -40% N ₂	6.65	1.135	29.2	3585	2103	6.81	145	6.28
JP10-O ₂ -60% N ₂	4.73	1.140	24.1	3316	1972	6.12	133	5.21
JP10-air	2.79	1.164	18.4	2843	1784	5.32	115	3.55

Table 2: Detonation CJ parameters and computed impulse for selected stoichiometric mixtures at 1 bar initial pressure and 300 K initial temperature.

List of Figures

1	Model predictions versus experimental data ³ for the impulse per unit volume. Filled symbols represent data for unobstructed tubes, whereas open symbols show data for cases in which obstacles were used. Lines corresponding to +15% and -15% deviation from the model values are also shown. * symbols denote high-pressure (higher than 0.8 bar), zero-dilution cases.	8
2	Specific impulse scaling with energy content. Model predictions versus effective specific energy content q for hydrogen, acetylene, ethylene, propane, and JP10 with air and oxygen including 0, 20%, 40%, and 60% nitrogen dilution at $P_1 = 1$ bar and $T_1 = 300$ K.	9
3	Variation of mixture-based specific impulse with initial pressure. Nominal initial conditions are $T_1 = 300$ K, stoichiometric fuel-oxygen ratio.	10
4	Variation of mixture-based specific impulse with equivalence ratio. Nominal initial conditions are $P_1 = 1$ bar, $T_1 = 300$ K.	11
5	Variation of mixture-based specific impulse with nitrogen dilution. Nominal initial conditions are $P_1 = 1$ bar, $T_1 = 300$ K, stoichiometric fuel-oxygen ratio.	12

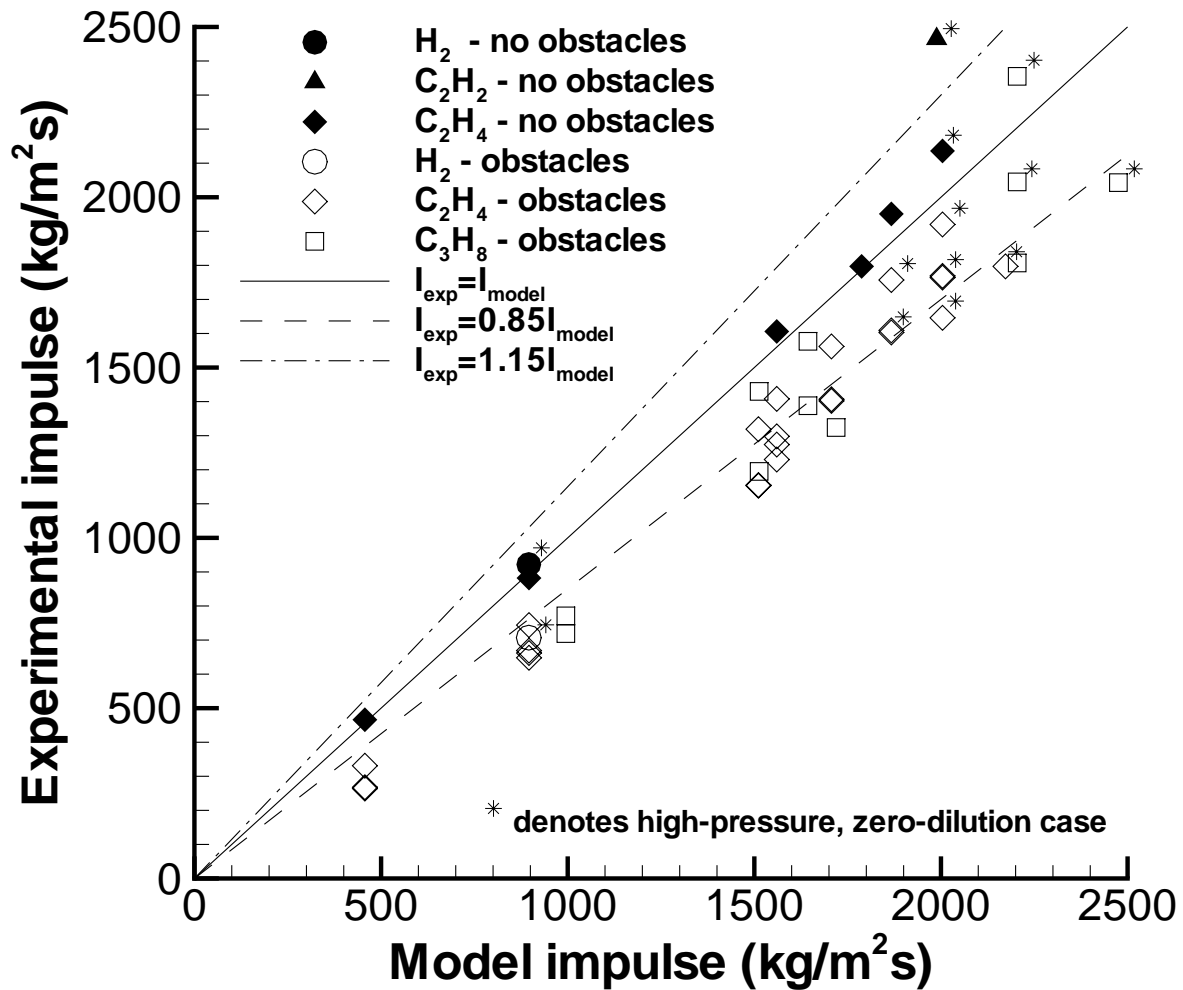


Figure 1: Model predictions versus experimental data³ for the impulse per unit volume. Filled symbols represent data for unobstructed tubes, whereas open symbols show data for cases in which obstacles were used. Lines corresponding to +15% and -15% deviation from the model values are also shown. * symbols denote high-pressure (higher than 0.8 bar), zero-dilution cases.

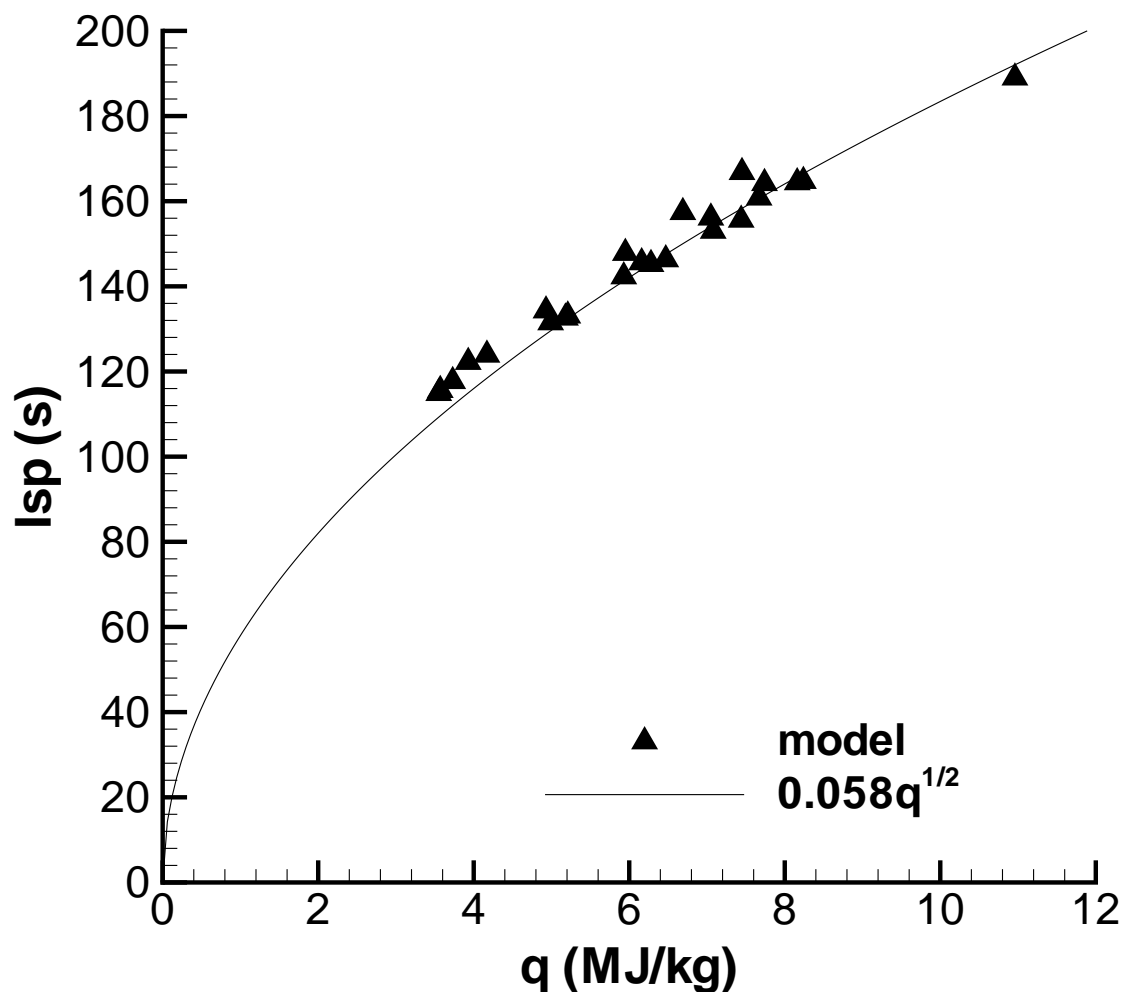


Figure 2: Specific impulse scaling with energy content. Model predictions versus effective specific energy content q for hydrogen, acetylene, ethylene, propane, and JP10 with air and oxygen including 0, 20%, 40%, and 60% nitrogen dilution at $P_1 = 1$ bar and $T_1 = 300$ K.

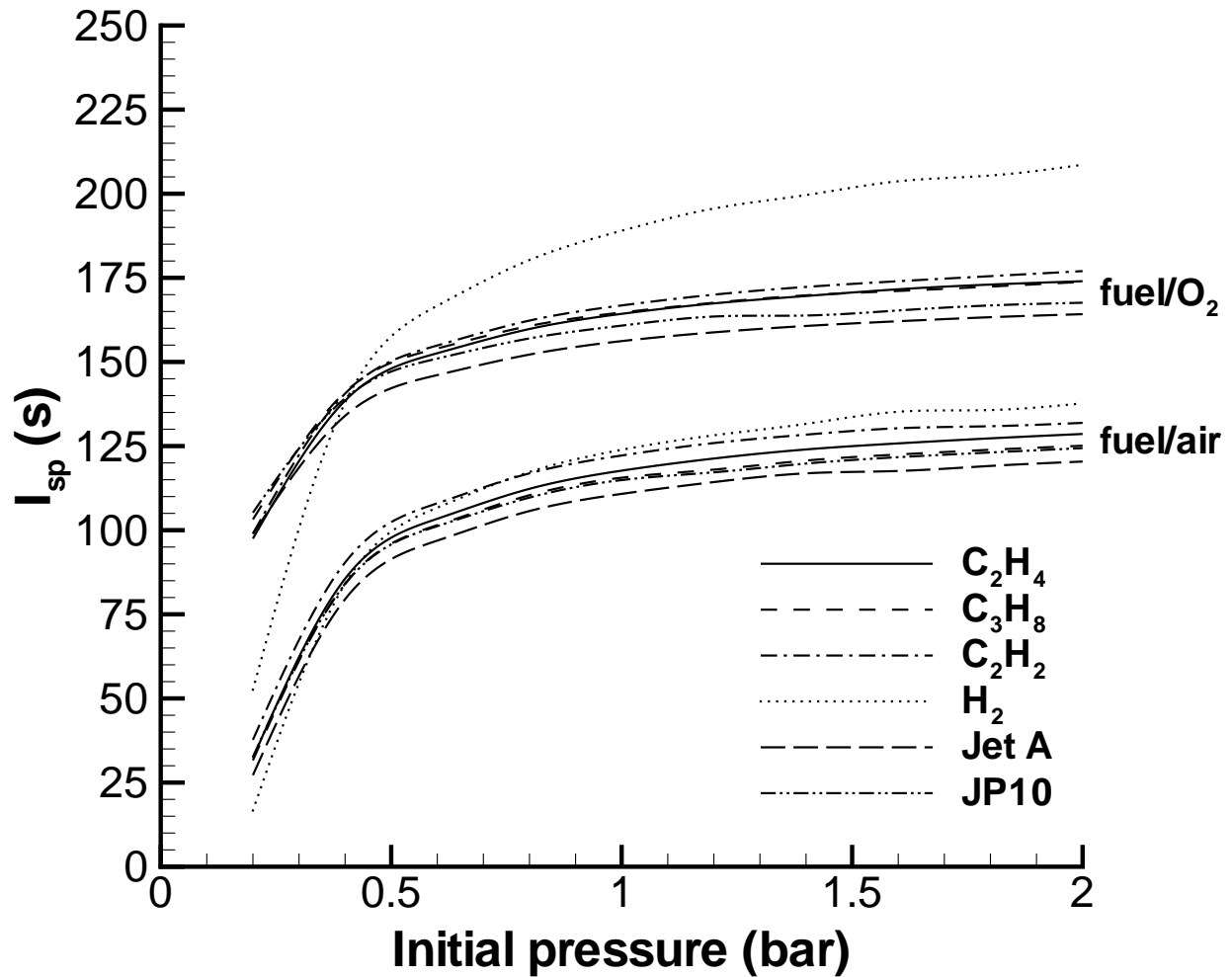


Figure 3: Variation of mixture-based specific impulse with initial pressure. Nominal initial conditions are $T_1 = 300$ K, stoichiometric fuel-oxygen ratio.

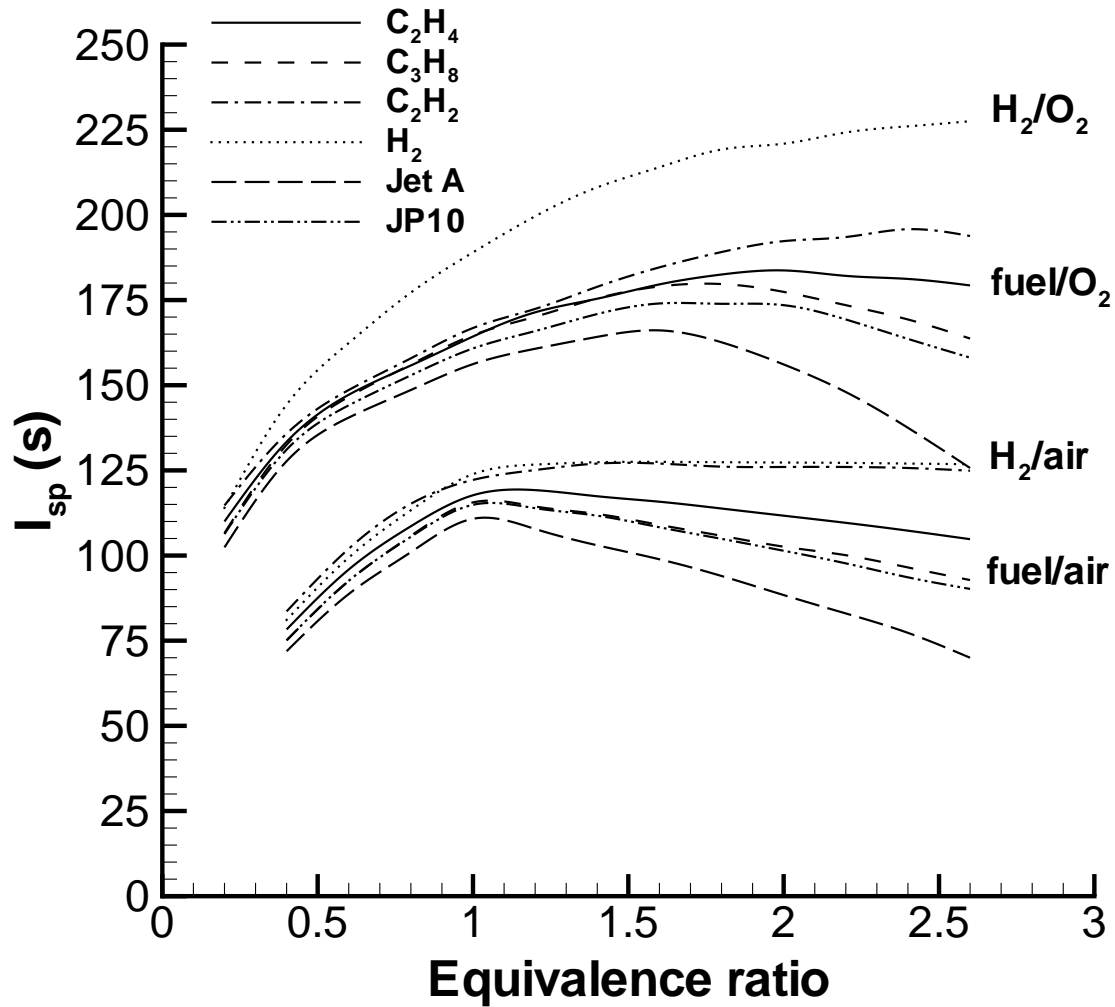


Figure 4: Variation of mixture-based specific impulse with equivalence ratio. Nominal initial conditions are $P_1 = 1$ bar, $T_1 = 300$ K.

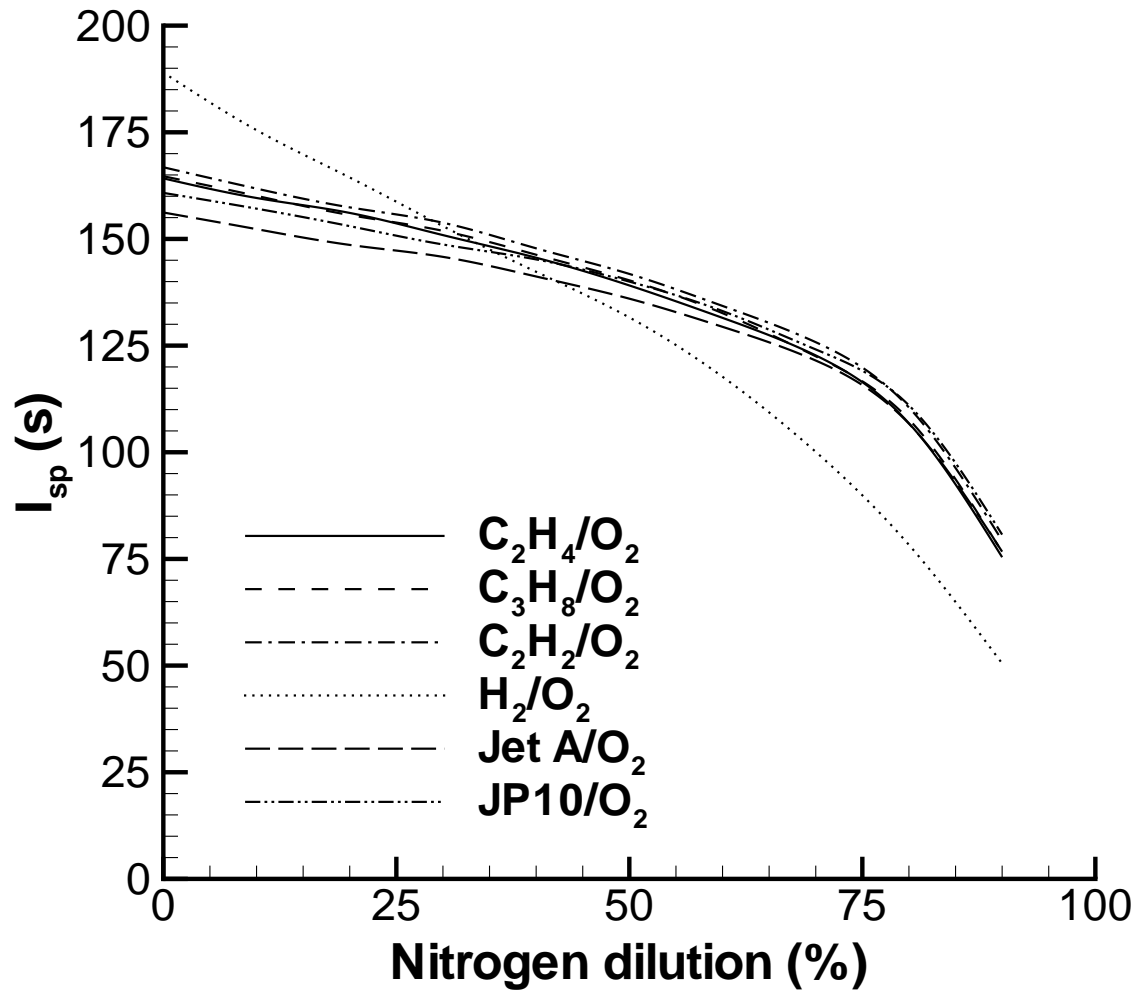


Figure 5: Variation of mixture-based specific impulse with nitrogen dilution. Nominal initial conditions are $P_1 = 1$ bar, $T_1 = 300$ K, stoichiometric fuel-oxygen ratio.